varian

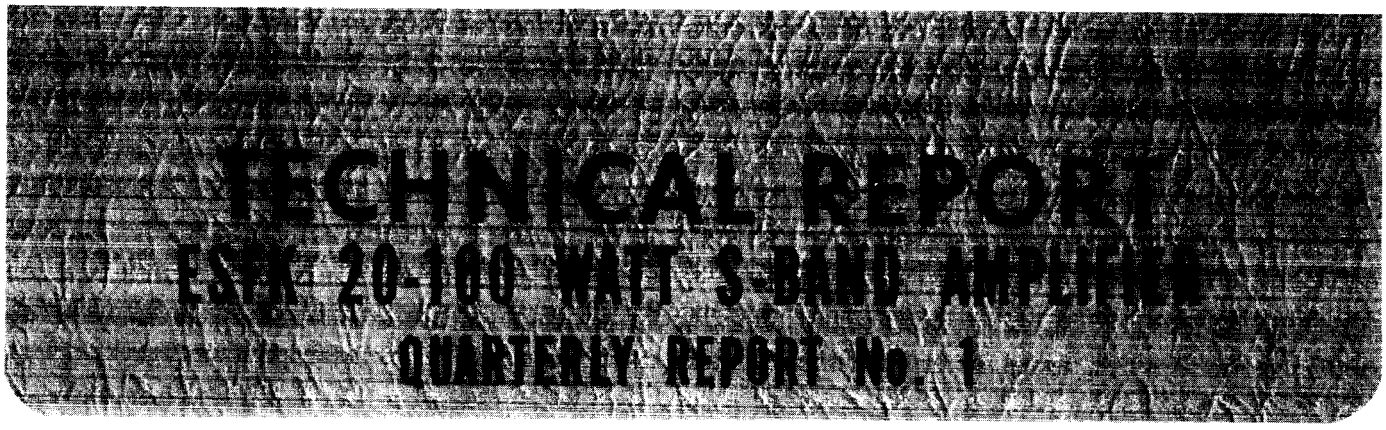

JPL CONTRACT No. 951105

APRIL, 1967

"This work was performed for the Jet Propulsion Laboratory, California Institute of Technology, sponsored by the National Aeronautics and Space Administration under Contract NAS7-100."

EIMAC division
301 industrial way
san carlos, california

BSFK 20-100 WATT S-BAND AMPLIFIER

QUARTERLY REPORT NO. 1

ERLING L. LIEN
ALBERT MIZUHARA

APRIL, 1967

JPL CONTRACT NO. 951105

"This work was performed for the Jet Propulsion Laboratory, California Institute of Technology, sponsored by the National Aeronautics and Space Administration under Contract NAS7-100."

by

Eimac®
DIVISION OF VARIAN ASSOCIATES
301 INDUSTRIAL WAY
SAN CARLOS, CALIFORNIA

NOTICE

This report was prepared as an account of Government-sponsored work. Neither the United States, nor the National Aeronautics and Space Administration (NASA), nor any person acting on behalf of NASA:

a. Makes warranty or representation, expressed or implied, with respect to the accuracy, completeness, or usefulness of the information contained in this report, or that the use of any information, apparatus, method, or process disclosed in this report may not infringe privately-owned rights; or

b. Assumes any liabilities with respect to the use of, or for damages resulting from the use of any information, apparatus, method, or process disclosed in this report.

As used above, "person acting on behalf of NASA" includes any employee or contractor of NASA, or employee of such contractor, to the extent that such employees or contractor of NASA, or employee of such contractor prepares, disseminates, or provides access to, any information pursuant to his employment with such contractor.

Requests for copies of this report should be referred to:

National Aeronautics and Space Administration
Office of Scientific and Technical Information
Washington 25, D. C.

Attention: AFSS-A

ABSTRACT

A 20 to 100 watt, S-band, electrostatically focused klystron having a radiation-cooled depressed collector for use in inter-planetary space-borne communication systems is presently under development. Although two klystrons have been built in the past which satisfied the power output and bandwidth (30 MHz at the -3 db points) requirements, the highest efficiency achieved was 38 percent at the 100 watt level - lower than the 45 percent required by the specifications. The 30 MHz bandwidth was achieved through the use of eight extended-interaction resonators which were stagger-tuned.

In order to achieve the 45 percent efficiency level, the existing program was redirected with new milestones.

This quarterly report describes the first major milestone of this 14 month efficiency improvement program: the design of a 5 - resonator, narrow band klystron, fabricated primarily to investigate the various efficiency improvement schemes. Small-signal gain calculations showed that a total of five resonators were required.

Presented in graphical form are the operating characteristics of the klystron such as rf efficiency and beam transmission as a function of the load conductance of the output resonator normalized to the beam conductance.

(REVIEW AND APPROVAL)

TABLE OF CONTENTS

TABLE OF CONTENTS (Continued)

LIST OF FIGURES

I. PRELIMINARY DESIGN

A. Computer Analysis of dc Beam

1. Purpose

One of the design areas thoroughly investigated was the periodic-electrostatic-focusing system used in the klystrons developed under this program. The purpose of the study was to find the most stable beam geometry in an eight-lens system.

2. The Computer Program

The digital computer program is able to calculate the electron trajectories, taking space-charge forces into account, of a dc beam through a given focusing system. The overall shape of the axially-symmetric beam is described by the program in two-dimensional form by sampling several electrons in the beam and computing their individual trajectories. Normally, 8 to 12 electrons are sufficient to fully describe a beam. The final solution is presented in printed as well as in graphical form; i.e., the trajectories are plotted to scale on graph paper having an r-z coordinate system. Also plotted for reference purposes are the lens electrode boundary and certain equipotential lines.

3. Lens Parameters

The lens model used in the analysis was identical to the one used in the last tube, tube 2a. The perveance of the beam was kept constant throughout the investigation at 0.72 microperveance. The variable parameter was the beam filling factor, defined as the ratio of beam-to-tunnel radii.

The investigation consisted of a systematic computation of various diameter beams through eight lens stages. Because of the limited capacity of the computer, the trajectories through only one lens stage could be calculated per run. The trajectory data at the output of each lens stage was then used as the input data for the next stage. This procedure was repeated through all eight lenses.

The filling factors studied, along with some relevant data, are given below for the first lens:

Filling Factor	V_{beam} (volts)	V_{lens} (volts)	V_{min} (volts)
0.65	3200	-600	1320
0.70	3200	-350	1373
0.75	3200	-100	1473
0.80	3200	+200	1569
0.90	3200	+700	1782

In all cases, the beam was injected into the first lens stage at an energy level corresponding to 3200 volts. V_{lens} is the dc potential (with respect to the cathode) at which the lens element must operate in order to focus the beam so identical radii exist at the entrance and exit planes of the first stage. This lens voltage was kept constant for all subsequent calculation involving the given filling factor. V_{min} is the lowest dc potential which any part of the beam achieves. It is located at the intersection between the transverse symmetry plane of the lens and the maximum beam radius. This potential is given with respect to the cathode voltage. A numerically larger (more positive) value is desirable here, as it represents a smaller level of voltage depression, and reduces the possibility of reflecting the slower electrons which necessarily exist in a modulated beam.

4. Results

0.65 filling factor

This is the filling factor used in tube No. 2a. The outermost electron, the one most subjected to the influence of spherical aberration, "ballooned out" at lens No. 6, crossed the axis twice, and collided into the drift tunnel after lens No. 7. The lowest potential level which this electron experienced was 760 volts.

0.70 filling factor

Except for "ballooning" of the outermost electron at lens No. 7, the beam traversed all 8 lenses without event. The value of V_{min} for this beam was 1111 volts.

0.80 filling factor

This beam exhibited the least amount of scalloping as it traversed the first seven stages. However, because of its higher filling factor, there is less overall clearance to begin with and the outermost electron did eventually collide with the drift tunnel at lens No. 8. As only seven lenses are used in an 8 resonator klystron, the plane of interception corresponds to the entrance plane of the collector, and is therefore inconsequential. The V_{min} for this filling factor is quite favorable, being 1480 volts.

0.90 filling factor

After traversing three lens stages, it became apparent that this very large filling factor allowed no margin between beam and tunnel beyond lens No. 3. The impracticality of this case discouraged further investigation.

In general, beams having 0.65 and 0.90 filling factors are not satisfactory. The 0.7 filling factor beam exhibits greater scalloping and potential depression than the 0.8 filling factor beam, but has more clearance than the 0.8 filling factor beam. However, both the 0.7 and 0.8 filling factor beams are more stable than the 0.65 or 0.9 filling factor beams. A 0.75 filling factor beam appears to be a reasonable compromise, offering stability and clearance.

B. Computer Analyses of a Simulated rf Modulated Beam

1. Purpose

In addition to the investigation of the periodic focusing system, the conversion of axial velocity to radial velocity by the last lens was studied.

Under modulated rf operation, the beam emerging from the penultimate cavity is velocity modulated and is composed of electrons with axial velocities higher and lower than the dc drift velocity. As these electrons travel on to traverse the last lens, they experience varying levels of radial-velocity modulation at the expense of axial-velocity modulation. This conversion process was investigated using the same computer program as that used previously to study electron trajectories.

2. Beam Models

The computer beam models studied have filling factors of 0.65 and 0.80. As approximately a 30 percent depth of modulation was assumed, this meant a swing of $\pm$ 1000 volts for a 3200 volt beam. Therefore, for each of the two filling factors, two initial velocities were used in the study corresponding to the lowest and highest electron energy

levels of 2200 volts and 4200 volts, respectively. Once again, only dc space charge was taken into account in the calculations and the beam at the entrance plane was assumed to be laminar with a homogeneous current distribution.

3. Results

The table below summarizes the computer results:

Energy level of electrons at injection	0.65 filling factor	0.80 filling factor
4200 Volts	Beam laminar and well focused.	Beam laminar and well focused.
2200 Volts	Severe chromatic aberration. Collision with output cavity tunnel.	Beam highly convergent. Shallow cross-overs. No interception.

For the case involving the fast electrons, because of the effectively lower beam perveance at 4200 volts, the beam remained well focused, laminar and nearly parallel even through the output cavity tunnel. This was true for both filling factors. For the case where the electrons are injected at 2200 volts -- representing the slowest electrons in a modulated beam -- the situation is radically different as the trajectory is very strongly influenced by the chromatic aberration of the lens. Since the focal length of the lens depends upon the electron energy -- i.e., the lower the energy, the greater the change in focal length -- electrons injected at 2200 volts leave the lens highly convergent. For a filling factor of 0.80, the beam converges to a minimum filling factor of 0.52 halfway down the output cavity, before it diverges and enters the collector. Crossovers of

trajectories do exist, but as they occur at a very shallow angle with respect to the axis, they are of little consequence. The beam transmission is 100 percent for this filling factor. However, for a filling factor of 0.65, the addition of spherical aberration produces a highly convergent beam with severe crossovers. Beam interception occurred starting at the supported drift tube and continued downstream as it rapidly diverged from its minimum diameter near the entrance plane of the output cavity.

Based on the above computer results, an rf modulated beam of 0.80 filling factor is preferred over the smaller 0.65 filling factor beam because it is more stable and is less likely to be intercepted.

C. Calculation of rf Radial-Velocity Modulation

1. Purpose

The degree of radial-velocity modulation produced by the penultimate and output resonator was calculated to obtain a first order approximation of the beam profile in the vicinity of the output end of the tube.

2. Mathematical Description

The axial and radial velocities resulting from the rf modulation process are expressed by the following terms:

$$v_z = - \frac{\eta}{v_o} V M_z (r_o) e^{j\omega t_o} \quad \text{(axial-velocity component)} \qquad (1)$$

$$v_r = - j \frac{\eta}{v_o} V M_z (r_o) \frac{\beta_e r_o}{2} e^{j\omega t_o} \quad \text{(radial-velocity component)} \qquad (2)$$

where: $\eta = \frac{e}{m}$ (ratio of electron charge to mass)

v_o = velocity of unmodulated beam

V = rf gap voltage amplitude

$M_z(r_o)$ = complex axial beam-coupling coefficient in the gap

β_e = phase constant corresponding to the electron velocity

r_o = initial beam radius

$\omega = 2\pi f_o$

t_o = entry time at the center of the gap

Hence, the radial-velocity modulation is seen to be 90^o out of phase with the axial-velocity modulation.

By defining

$$\left|v_z\right| e^{j\theta} = - \frac{\eta}{v_o} V M_z (r_o), \tag{3}$$

Eqs. 1 and 2 above may be written as

$$v_z = \left|v_z\right| e^{j(\omega t_o + \theta)} \tag{4}$$

$$v_r = j \frac{\beta_e r_o}{2} \left|v_z\right| e^{j(\omega t_o + \theta)} \tag{5}$$

Considering only the real part of the above equations, we get

$$v_z = \left|v_z\right| \cos (\omega t_o + \theta) \tag{6}$$

$$v_r = - \frac{\beta_e r_o}{2} \left|v_z\right| \sin (\omega t_o + \theta) \tag{7}$$

Eqs. 6 and 7 are shown plotted in Fig. 1.

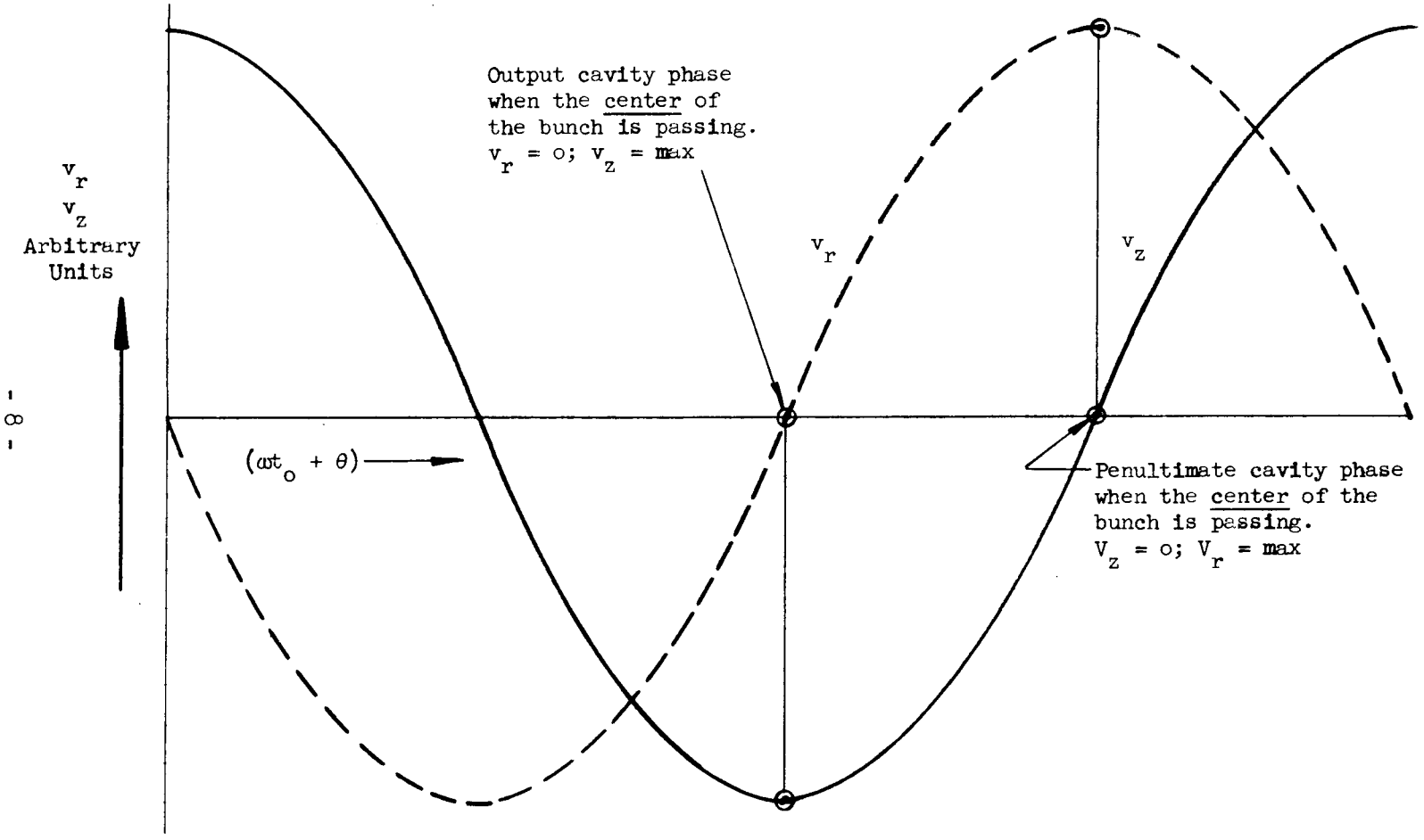

Fig. 1 - Plot showing phase relationship between axial and radial rf velocity components as a function of the electron entry phase.

In the case of the penultimate resonator, the radial-velocity modulation of the center electron of the bunch as it passes through the middle of the gap is positive (defocusing). At the same instant, the axial field is zero, but passing from a retarding to accelerating phase. For this latter case, the approximate increase in beam spread due to the rf radial-velocity modulation is 2 degrees. If we assume the deflection originates at the center of the penultimate cavity, this 2 degree increase results in a 17 percent increase in the diameter of the beam minimum at the center of the output gap.

For the case of the output cavity alone, the radial-velocity modulation is zero when the axial-velocity modulation is at a maximum. Consequently, at center frequency operation the resultant beam spread beyond the output gaps is due to the space-charge forces alone. If we assume for this calculation, the effective bunched beam perveance to be close to 3 microperveance, the beam spread angle due to the space charge alone is 6 degrees. Added to this must be the penultimate cavity radial-velocity modulation given above. If it is assumed that the beam spread starts at the middle of the output cavity, the beam diameter at the middle of the exit gap of the output cavity is about 0.200 inch increasing to about 0.230 inch just beyond the downstream nozzle. Based on the above calculations alone, it is evident that the output cavity tunnel geometry used in tube No. 2a is marginal from the beam transmission point of view since the downstream nozzle tunnel is 0.230 inch in diameter. However, as the rf modulating process is an extremely complex one -- even more so for an electrostatically focused klystron -- numerous simplifying assumptions

are necessarily involved. Therefore, the numerical results are useful primarily as a guide. The refinement in tunnel geometry design must rely heavily on experimental results.

D. Output Cavity Cold Test Investigation

Based on the rf radial-velocity modulation calculations, it was decided to increase the tunnel diameter. The cold tests were made using a fixed, supported-drift-tube-diameter of 0.240 inch, with various upstream nozzle diameters ranging from 0.205 to 0.240 inch. The downstream nozzle diameter varied from 0.230 to 0.260 inch. The R/Q for these cavities ranged from 190 to 210 ohms. The gap spacings were fixed at 0.051 inch. Other tests in which the gap spacings were varied showed that the change in R/Q with gap spacing is about 1.5 ohms per mil. It was also found that the supported-drift-tube diameter affects the R/Q more than the upstream or downstream nozzle diameters. Generally speaking, the smaller the supported-drift-tube diameter and the larger the gap spacings, the higher the value of R/Q.

The final geometry of the output cavity used for tube 3s is

upstream nozzle	.230 inch diameter
supported nozzle	.230 inch diameter
downstream nozzle	.260 inch diameter
gap spacings	.070 inch per gap

These diameters were chosen to allow the modulated beam to clear the output cavity with little or no interception.

E. Small-Signal Gain Calculation

The minimum number of resonators which a klystron utilizing a dual

penultimate resonator system requires is four. The table below gives the values for resonator order, function, R_{sh}/Q, and Q-factors. These parameters were used in the gain calculations.

Resonator	Function	R_{sh}/Q	Q_o	Q_L
#1	input	193Ω	346	190
#2	antepenultimate	204Ω	314	—
#3	penultimate	204Ω	373	—
#4	output	230Ω	1720	51

The normalized spacing $\beta_e \ell$ is 7.28 radians between all resonators. The antepenultimate and penultimate resonators are functionally used together to simulate a single penultimate cavity having a higher R_{sh}/Q. For this four-resonator case, the small-signal gain calculations performed by a computer showed the gain to be well below the required 30 db as dictated by the rf drive level available from the test instrument. This is because both resonators No. 2 and 3 must be detuned about 1.5 percent above band center, thereby contributing little or nothing to the gain mechanism. At least 30 db of small-signal gain is necessary to achieve the minimum saturation gain of 24 db, as the rf driver used during hot test is not able to generate more than about 0.5 watt of power. Therefore, it is clear that four resonators are insufficient.

With the addition of a fifth resonator between resonators 1 and 2, an immediate increase in small-signal gain to 38 db or more is obtained. This additional resonator unloaded Q and R_{sh}/Q were 460 and 212, respectively. The gain for several possible tuning patterns to be used in the testing of the tube were calculated and the results are given below. The tuning of the antepenultimate and penultimate resonators with respect to the operating frequency has a dominate effect on the efficiency. Several tuning patterns were therefore tried.

Case	Small-Signal Gain	MHz Deviation From Center Frequency				
		Cavity 1	Cavity 2	Cavity 3	Cavity 4	Cavity 5
1	42 db	0	0	26	26	0
2	38 db	-12	0	16	16	0
3	43 db	-12	0	5	16	0
4	39 db	0	0	42	42	0
5	38 db	0	0	67	42	0

In Case 1 above, all cavities are set to f_o except for the antepenultimate and penultimate cavities. These are set 26 MHz higher based on a large - signal calculation which showed this tuning pattern to be the one yielding the highest efficiency. The gain is 42 db. In Case 2, cavities No. 3 and No. 4 are brought in closer to the operating frequency. Resonator No. 1 is placed 12 MHz below f_o. This is imposed by the tuning limit of the actual resonator fabricated for tube No. 3s. The consequence of this is that the response curve becomes broader, and the gain is decreased. Case 3 is with cavity No. 3 tuned in close to band center with cavity No. 4 left alone to simulate operation with a single penultimate cavity. As a result of bringing cavity No. 3 in toward band center, the gain is 43 db. Case 4 is simply an extension of Case 1, with both penultimate cavities tuned an additional 16 MHz above that of Case 1. The decrease in gain is only 3 db. Case 5 is with Cavity No. 3 moved another 25 MHz to a total of 67 MHz from band center. The gain is essentially the same as for Case 4, as cavity No. 3 is tuned so far out of the band that it is essentially inoperative as a resonator and for all practical purposes may be replaced by a drift tunnel.

Based on the above computer calculations, at least 5 resonators are required with the resultant gain being about 40 db. Four resonators are insufficient.

II. SHORT TUBE DESIGN

A. Design Changes

The preliminary design information given above was used as the basis for several design changes in tube No. 3s. The table below shows these changes in term of tubes No. 2a and 3s.

	Tube No. 2a	Tube No. 3s
Beam filling factor	0.65	0.75
Beam diameter	0.130 in.	0.150 in.
Cathode diameter	0.333 in.	0.385 in.
Buncher tunnel diameter	0.200 in.	0.200 in.
No. of resonators	8	5
No. of lenses	8	4
Lens between gun and resonator No. 1	Yes	No
Modulating anode	Yes	No
Lens, method of support	Mechanically clamped	Brazed
Lens feed insulator path length	.125 in.	.250 in.
Lens diameter	All lenses 0.357 in.	Lens Nos. 1 to 3 0.357 in. Lens No. 4 0.384 in.

B. Gun Scaling

The beam filling factor was increased from 0.65 to 0.75 by increasing the beam diameter to 0.150 inch while keeping the tunnel diameter unchanged at 0.200 inch. To generate this larger beam diameter without changing the perveance, all linear gun dimensions were scaled by the factor $\frac{0.75}{0.65} = 1.153$. (When operated at 3 KV, the cathode current was 0.127 amp.; the corresponding perveance is 0.74 microperveance).

C. Lens Scaling

With regard to the lens voltage, the computer analyses of the dc beam showed the optimum lens voltage for a lens system having a beam filling factor of 0.75 and a lens diameter of 0.357 inch to be -100 volts with respect to the cathode potential. Since it is preferable, when using separate lens power supplies, to have the lenses slightly negative with respect to cathode to prevent electron interception, the lens diameters for the first three lenses were left the same as that used previously in tube 2a. The exception to this is lens No. 4 -- located between the penultimate cavity and the output cavity -- which operated more positive than the other lenses by 400 volts in tube No. 2a. To be able to operate this lens in the negative region, it was necessary to enlarge the internal diameter from 0.357 inch to 0.384 inch. The design voltage for each of the lenses is compared to the actual operating voltage in the table below for tube No. 3s.

Lens No.	Design Voltage*	Actual Voltage*
1	-100 V	-200 V
2	-100 V	-200 V
3	-100 V	-400 V
4	-100 V	-200 V

* With respect to a cathode voltage of -3 kv.

These measured values do not coincide exactly with the design values since the latter values were based on a dc unmodulated beam. Because of the compensating adjustment made to the diameter of lens 4, its operating voltage is identical to that of lenses 1 and 2. It appears as if a stronger focusing action is required on lens 3 to optimize the beam shape further down stream.

D. Input Resonator

The input resonator loaded Q in tube 2a was 13 in order to present a low VSWR across the 30 MHz band. Since bandwidth was not a requisite condition for the short tube, whereas gain was, the short tube was designed with a Q_L equal to 190. Coupling was achieved as before (in tube 2a) with a probe coupled to the radial field of the helical resonator.

E. Output Resonator

The output resonator design was based on the best available data from the preliminary design phase covered earlier in this report. A compromise tunnel configuration was arrived at which was small enough to yield a high value of R_{sh}/Q and yet large enough to provide adequate clearance between tunnel and beam. The various parameters are shown below compared to those for tube 2a:

Output Resonator	Tube 2a	Tube 3s
Number of gaps	2	2
Upstream gap spacing	.058	.065 inch
Downstream gap spacing	.062	.070 inch
Upstream nozzle diameter	.205	.230 inch
Supported tunnel diameter	.215	.230 inch
Downstream nozzle diameter	.230	.260 inch
R_{sh}/Q	254	230 ohms
Q_L	47.5	51

A 10 percent reduction in R_{sh}/Q resulted from enlarging the drift tube tunnel, despite the increase in gap spacings to offset the reduction. Except for the differences noted above, the output cavity was constructed in the same manner as that for tube No. 2a.

F. Test Results

1. Introduction

As explained in the previous sections of this report, the purpose of making the short, five-cavity tube was to establish the maximum efficiency obtainable. The basic set of tests performed on the tube were therefore the measurement of the conversion efficiency and the overall efficiency under depressed collector operation. Measurements necessary for a detailed understanding of the factors limiting the rf efficiency and the radiation cooling efficiency were also performed. These tests were performed with the voltage of lens No. 4 (last lens) adjusted first for optimum beam transmission to the collector and later for optimum output power. No measurement was done of the gain-bandwidth response of the tube. However, the rf efficiency was measured as a function of the load conductance of the output resonator. This result can be used in the prediction of possible trade-offs between output cavity bandwidth and rf efficiency.

A fixed frequency-tuning pattern of the four-buncher resonators with respect to the operating frequency was used throughout the tests. The frequencies selected for resonators No. 3 and No. 4 (which have the main effect on efficiency), was based upon a compromise between possible penultimate resonator frequency drift at the 100 watt power level and optimum rf beam current at the output resonator. The best compromise was obtained with resonators No. 3 and No. 4 tuned to the same frequency of 37 MHz above the operating frequency. The optimum efficiency at an operating voltage of 3 kv was obtained with 30 MHz detuning. This is in good agreement with the optimum detuning of 26 MHz predicted by the large-signal analyses at the start of this development program.

2. Analyses of Test Data

The measured conversion efficiencies and beam transmissions are shown as a function of the normalized load conductance G_L/G_O, for beam voltages of 3 kv and 2 kv in Figures 2 and 3, respectively. The theoretically predicted efficiencies at the two operating voltages are included for comparison. An interaction impedance $(R_{sh}/Q) = 230$ ohms for the output resonator was used in the calculation of the theoretical curves. The loading required to obtain minimum -3 db bandwidths of 20 MHz and 30 MHz for a 1.2:1 load variation in the output cavity, correspond to loaded Q-factors of $Q_L = 96$ and $Q_L = 64$, respectively. These points are noted on the abscissa in Figures 2 to 5.

It is seen from Fig. 2 that the predicted efficiency is very close to the observed efficiency for heavy loading of the output resonator when the voltage of the last lens is optimized for output power. The measured efficiency becomes progressively lower than the expected value for lighter loads. This can be explained by the increased beam interception associated with the increased rf output gap voltages for the lighter loads.

The conversion efficiency for $Q_L = 64$ is approximately 30 percent. This would be sufficient for obtaining an overall efficiency of 45 percent if full beam transmission could be maintained under depressed collector operation (the collector can be depressed to about 2/3 of the beam voltage). This, however, cannot be hoped for. Adjusting the lens voltage for optimum output power results in a beam which is very close to the drift-tube walls. This inherently results in beam interception. The adjustment for optimum output power is actually a

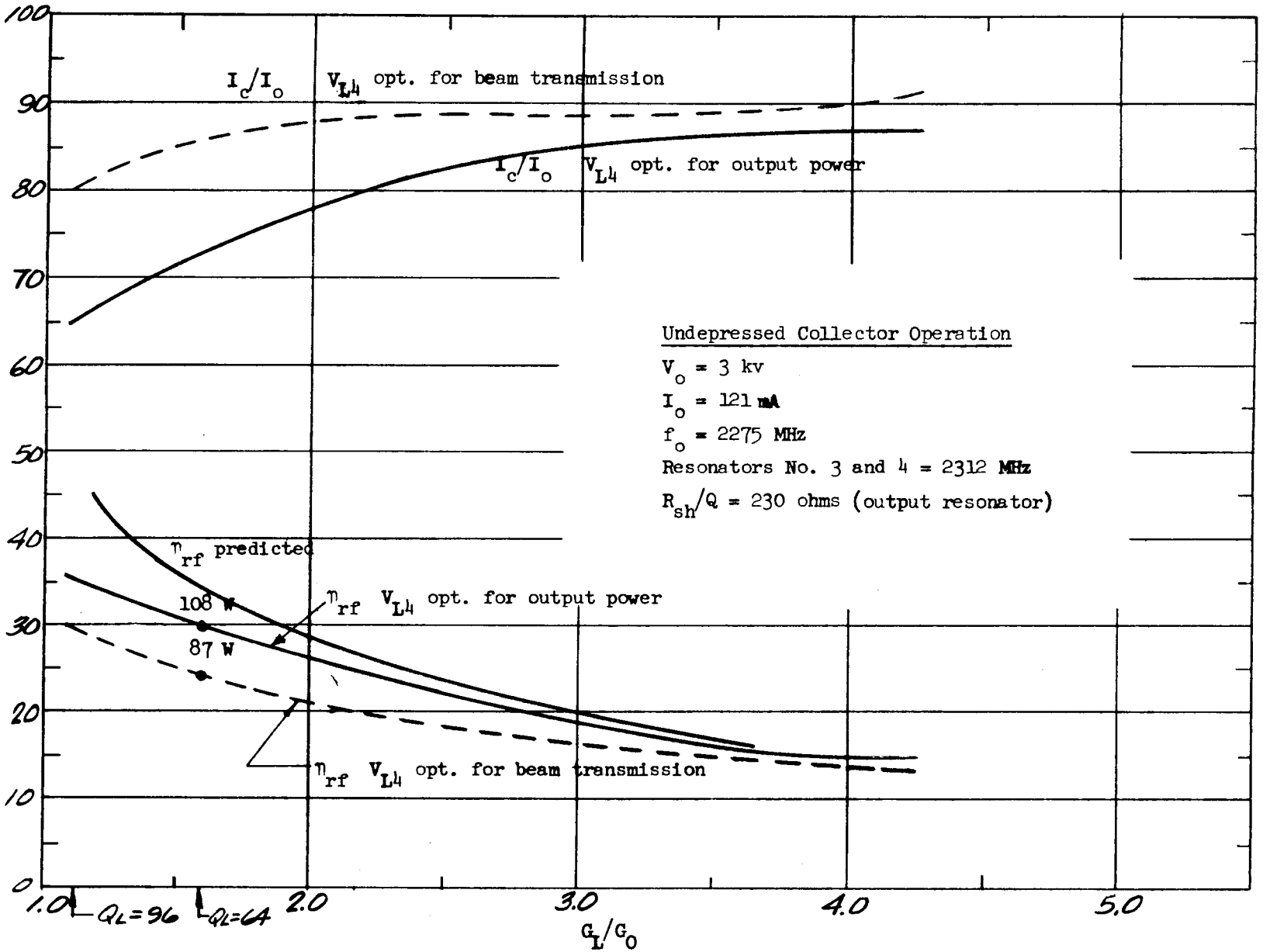

Fig. 2 - Measured beam transmission and conversion efficiency as a function of normalized load conductance. Shown also is the predicted efficiency.

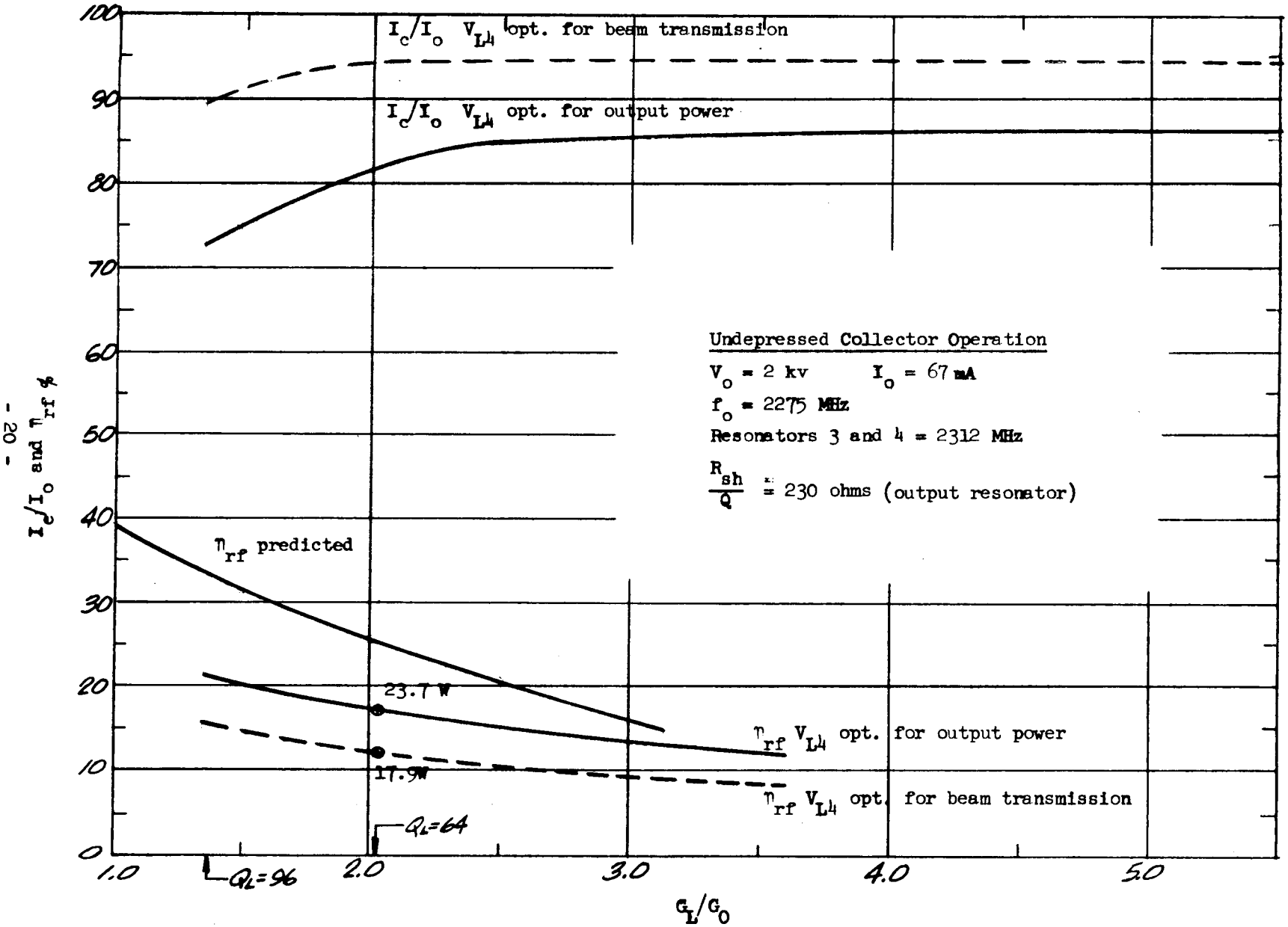

Fig. 3 - Measured beam transmission and conversion efficiency as a function of normalized load conductance. Shown also is the predicted conversion efficiency.

compromise between beam coupling to the resonator (requiring a large beam diameter) and beam interception. An optimum beam transmission can therefore only be obtained with some compromise in the conversion efficiency.

The measured output power for $Q_L = 64$ is 108 watts. Since the input dc power is constant, the output power for the other loads varies according to the conversion efficiency. It is seen that an increase in conversion efficiency can be obtained with some sacrifice in bandwidth (lighter load).

The measured beam transmission is 100 percent under dc operation. Beam interception is induced under rf operation, being partly produced by the radial modulation of the beam in the last buncher resonator and partly produced by the radial rf fields in the output resonator. The relative contribution of the two factors is evaluated by comparing the beam interception when the output resonator is heavily overloaded (small rf fields in the output) with that when it is normally loaded.

As shown in Fig. 2, for a beam voltage of 3 kv and a heavily overloaded resonator, the beam transmission under rf conditions is 86 percent when the last lens is adjusted for optimum output power; and, approximately 90 percent when the last lens voltage is adjusted for optimum transmission. For a loaded Q-factor $Q_L = 64$ of the output resonator, the transmission drops to 74 and 87 percent for the two aforementioned operating conditions of the lens. Thermal measurements of the collector heat show that when the collector is not depressed, the dominant intercepted electrons are primary electrons having an average energy resulting from the dc energy minus the rf extracted energy. The beam interception will, therefore, degrade the overall radiation cooling efficiency and should be minimized.

For a beam voltage of 2 kv (Fig. 3) the measured conversion efficiency is significantly smaller than the predicted value (for optimized buncher). This is partly due to the fact that the frequency of the penultimate resonators are not optimized for this power level. The measured conversion efficiency for $Q_L = 64$ (30 MHz, -3 db bandwidth operation) with the last lens optimized for output power is 17 percent and corresponds to an output power of 23.7 watts. When optimized for beam transmission, the efficiency and power output are 13 percent and 17.9 watts, respectively.

As shown in Fig. 2, the measured conversion efficiency when the last focusing lens is adjusted for optimum beam transmission is significantly smaller than the conversion efficiency obtained when the lens voltage is adjusted for optimum output power. In order to achieve the highest possible combination of beam transmission and conversion efficiency in future tube design, it is necessary to understand in detail the efficiency-reducing mechanism involved.

There are several factors which may contribute to the observed behavior. For one, the average beam diameter in the output cavity is most likely larger when the last lens voltage is adjusted for maximum output power than when it is adjusted for optimum beam transmission. This larger diameter beam yields maximum coupling to the rf field of the interaction gaps. Consequently, both the induced currents in the resonator gaps and the output power will be largest in this case.

Another, more speculative mechanism which might play an important role, is outlined below. The computer analyses of a simulated rf modulated beam being focused, showed that a large

chromatic lens aberration is introduced when the potential depression in the lens region is large. The lowest velocity electrons are given a large deflection and may be intercepted in the beam entrance portion of the resonator for low lens voltages. When the lens voltage is adjusted for optimum output power, the beam interception is predominantly in the exit region of the resonator. The intercepted current is composed of both originally high- and low-velocity electrons. As the lens voltage is decreased, the interception region of the low-velocity electrons are gradually shifted toward the entrance of the resonator, while the transmission of the originally higher-velocity electrons are improved. The overall beam transmission is increased, but the rf beam current and output power are reduced. The reduction of the output power tends to preserve the beam transmission by virtue of the reduced radial rf-velocity-modulation.

It is expected that a deeper insight into the problem will be gained through testing of the electron beam under rf conditions in the electron beam analyzer. If the predominant cause of the reduction in conversion efficiency for optimum beam transmission is the decreased rf coupling coefficient, the efficiency may be partly restored by reducing the beam tunnel diameter.

The measured efficiency and beam transmission under the depressed collector operation is shown as a function of the normalized load conductance G_L/G_0 for 3 kv and 2 kv beam voltages in Fig. 4 and Fig. 5, respectively. To determine the practical limit for collector depression, the collector potential was reduced to the lowest value before traces of regeneration effects could be observed, and then backed off to allow a margin of safety. The percentage depression of

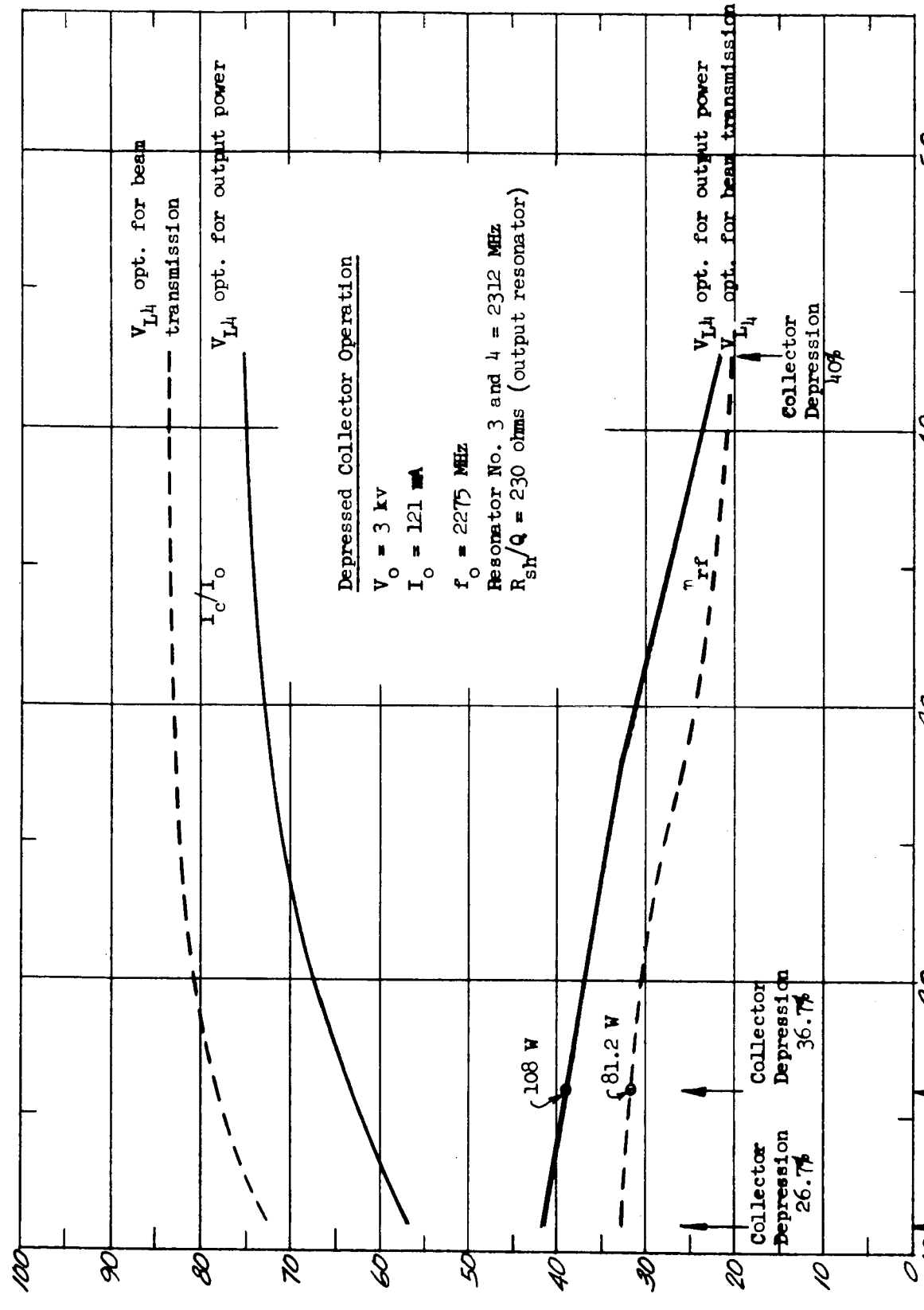

Fig. 4 - Measured beam transmission and depressed collector efficiency as a function of normalized load conductance.

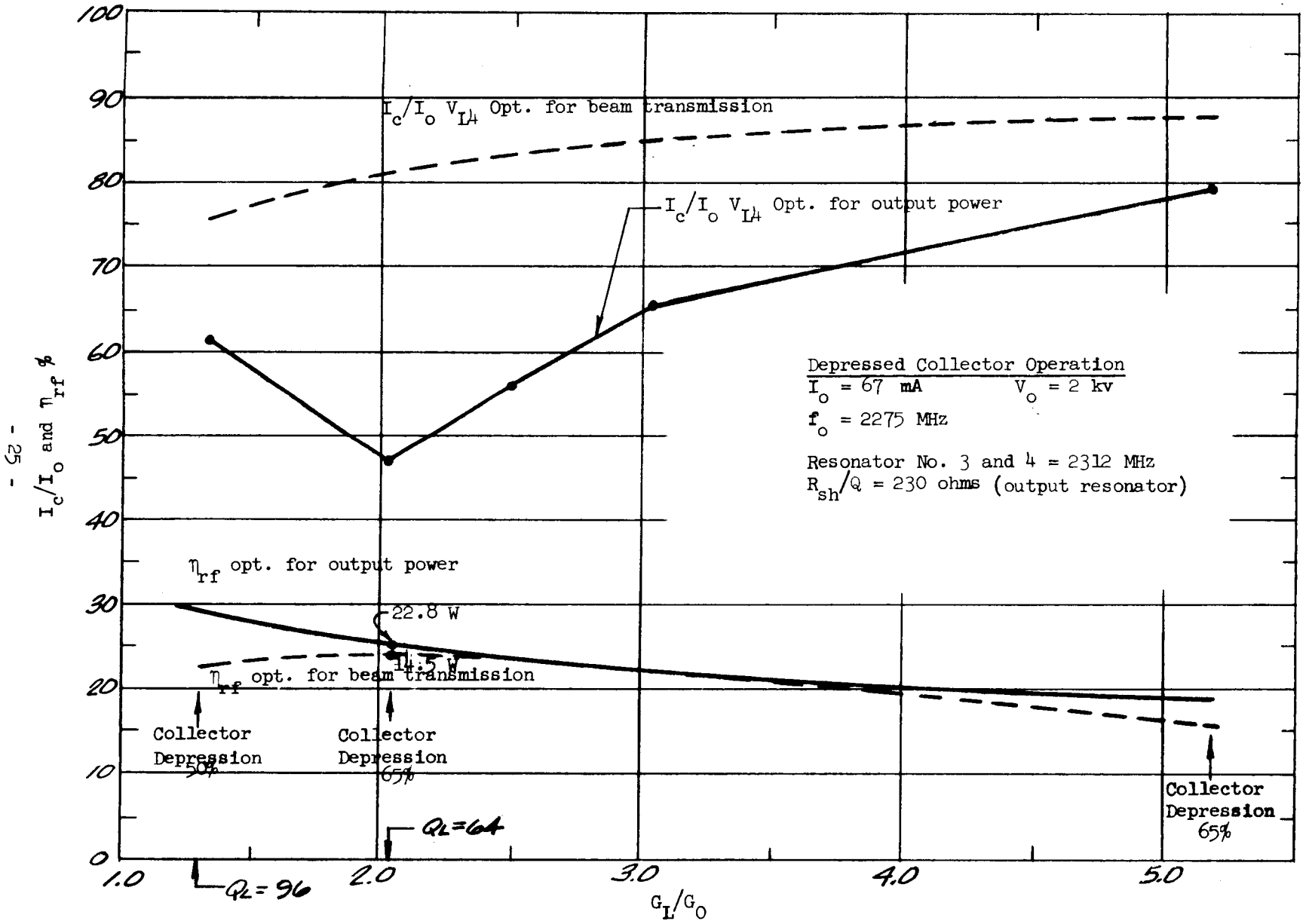

Fig. 5 - Measured beam transmission and depressed collector efficiency as a function of normalized load conductance.

the collector voltages below the beam voltage are indicated in the figures. The heater power is not included in the efficiency values because its design is still experimental.

At a beam voltage of 3 kv, and with the load adjusted for 30 MHz bandwidth, (Q_L = 64) the depressed collector efficiency is 38 percent when the last lens voltage is optimized for output power; and 32 percent when the lens voltage is optimized for beam transmission (Fig. 4). The corresponding values for a 20 MHz bandwidth is 41 and 33 percent, respectively.

The beam transmission is lower when operating with the collector depressed. The additional body current has been identified as consisting mainly of low-velocity secondary electrons released from the collector. Because of the increased beam diameter and output cavity tunnel diameter used in this tube, the beam is undoubtedly colliding with the collector near the opening, and generating secondary electrons. In addition, because of the larger beam diameter, the suppressor lens design was no longer optimized for suppressing secondary electrons. It is expected that improvement of the collector and suppressor lens design will eliminate the secondary electron problem.

For 2 kv beam voltage and Q_L = 64, (Fig. 5) the depressed collector efficiency is 26 percent for optimized output power and 24 percent for optimized transmission.

As indicated earlier in this section, trade-offs can be made between overall efficiency, beam transmission and radiation cooling efficiency. The dominant design parameter affecting the ultimate compromise design is the focal length of the last focusing lens

(lens No. 4). The focal length of this lens can be varied and thus experimentally optimized by changing its voltage. This change in lens voltage may be subsequently translated into an equivalent change in lens geometry.

In order to get a mapping of the possible trade-offs, the overall efficiency, the beam transmission and the collector thermal power dissipation were measured as a function of the last lens voltage (lens No. 4). This was done for several operating conditions of the tube. The most pertinent results are shown in Figs. 5 and 6. The rf efficiency, the collector current I_c to cathode current I_o ratio, and the thermal power of the collector W_c to total thermal power in the tube W_T ratio are plotted as a function of the lens No. 4 voltage V_{L4}. The total thermal power W_T is defined as the dc input power into the tube (power supply power) minus the rf output power. The percentage of the heat which can be expected to be disposed of by radiation from the collector is found by multiplying W_c/W_T by the radiation cooling efficiency of the collector which is approximately 0.8.

A beam voltage of 3 kv was used for these tests. The loaded Q-factor of the output resonator is $Q_L = 96$ in Fig. 6 and $Q_L = 64$ in Fig. 7. The tube was operated both with optimum collector depression, Figs. 6b and 7b and with no collector depression, Figs. 6a and 7a. The indicated rf efficiencies (excluding heater power) are the overall efficiency for depressed collector operation and the conversion efficiency for no collector depression. It is seen from Figs. 6 and 7 that the rf efficiency is a relatively slowly varying function of the lens voltage around the optimum efficiency point.

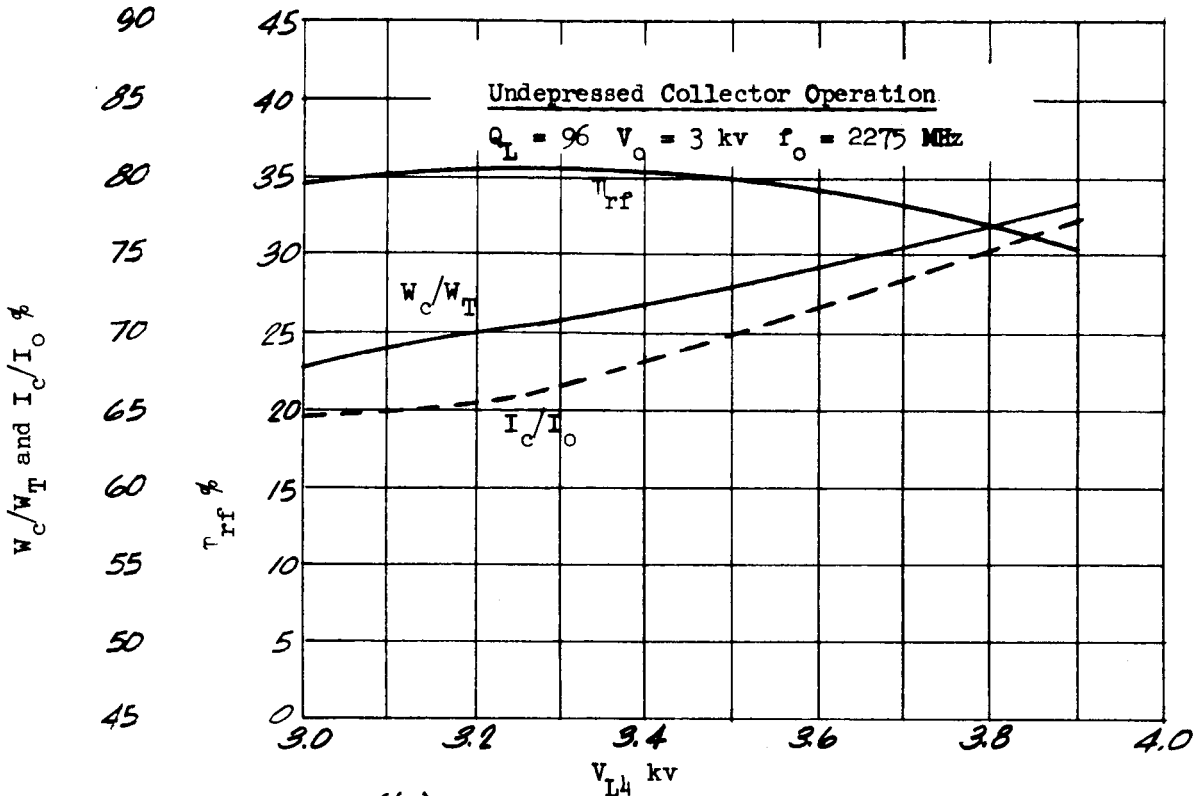

Fig. 6(a) - Beam transmission, conversion efficiency and collector thermal efficiency as a function of V_{L4}.

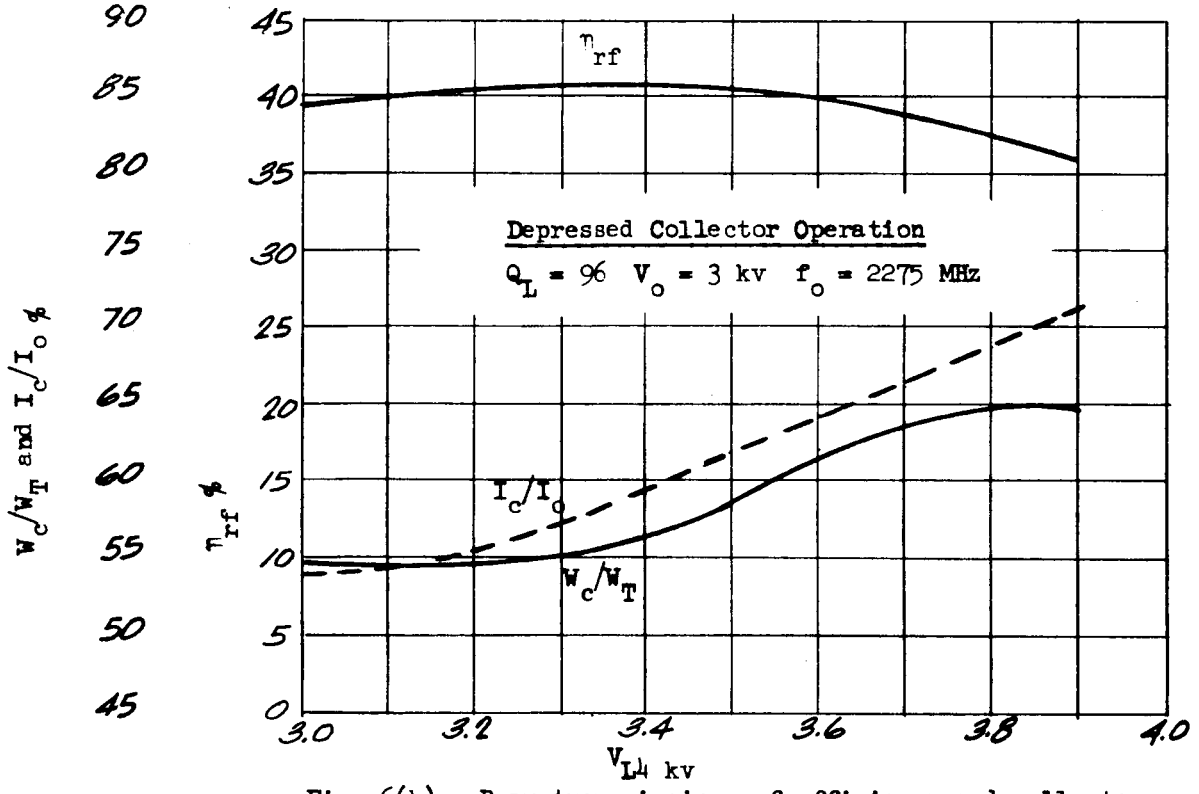

Fig. 6(b) - Beam transmission, rf efficiency and collector thermal efficiency as a function of V_{L4}. Collector is depressed 26.7 percent.

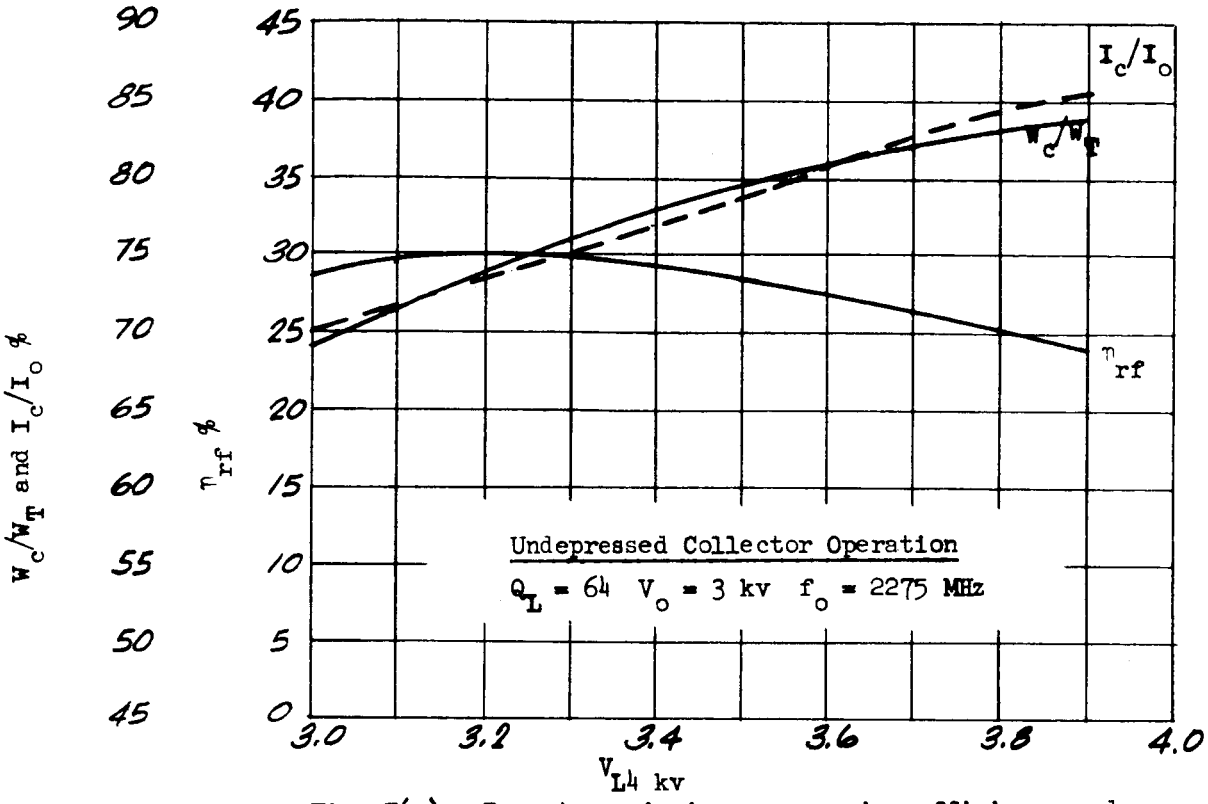

Fig. 7(a) - Beam transmission, conversion efficiency and collector thermal efficiency as a function of V_{L4}.

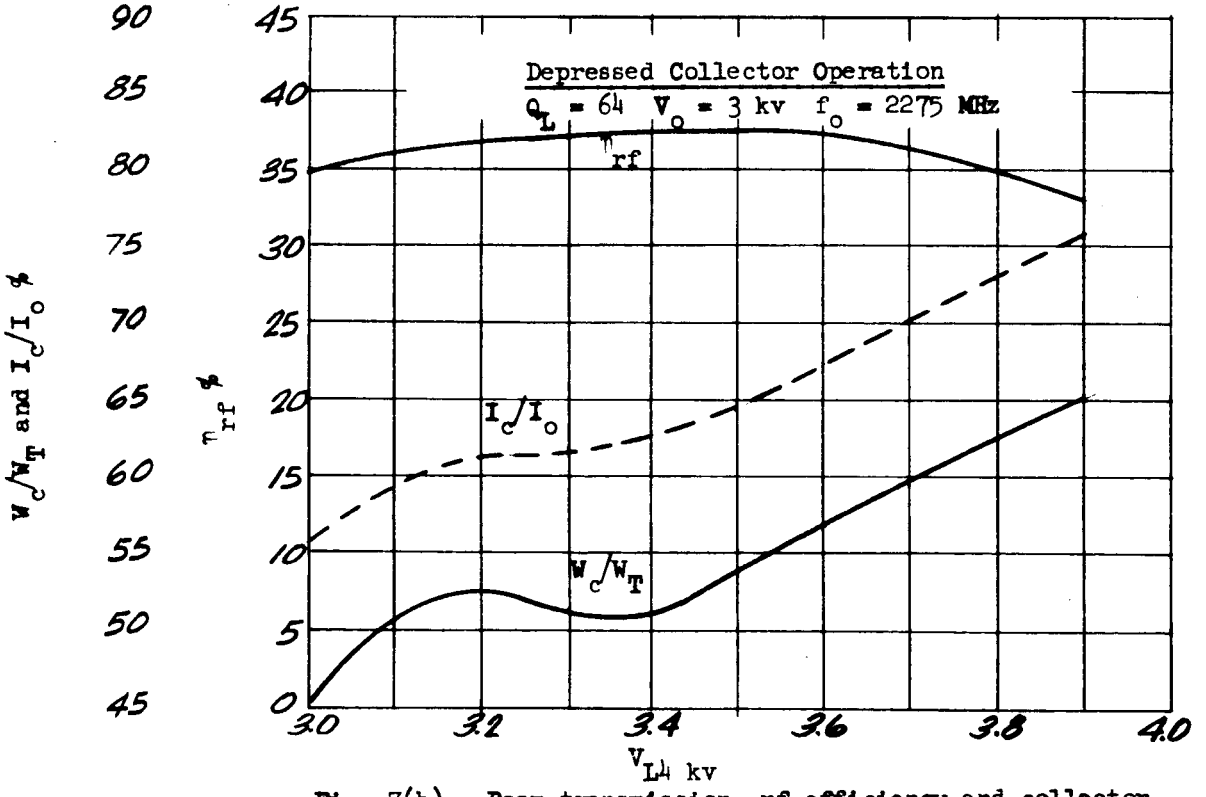

Fig. 7(b) - Beam transmission, rf efficiency and collector thermal efficiency as a function of V_{L4}. Collector is depressed 36.7 percent.

The point of optimum overall efficiency under depressed collector operation is slightly displaced toward the higher lens voltages compared to the voltage for optimum conversion efficiency. The reason for this is the improved beam transmission resulting from the higher lens voltages. The optimum lens voltage for rf efficiency seems to be independent of the loading of the output resonator.

A significant improvement in I_c/I_o and W_c/W_T can be obtained with a relatively small sacrifice of the rf efficiency. The value of W_c/W_T under depressed collector operation is smaller than the desired value of 75 percent needed for 60 percent collector radiation cooling efficiency. However, an improvement in W_c/W_T can be achieved (as well as in the overall rf efficiency) by elimination of the previously described problem with the release of secondary electrons from the collector.

III. BEAM ANALYZER EXPERIMENT

The purpose of this phase of the program is to investigate the beam with a pin hole target at the entrance to the output cavity. The beam analyzer itself is a large, vertical, cylindrical vacuum chamber connected to three vac-ion pumps. The klystron is mounted vertically, gun end up. The tube going into the chamber will consist of only the gun and buncher cavities. The output cavity, collector and appendage pump are removed from the klystron. A specially designed end plate with the same configuration as the upstream wall of the output cavity is used to replace the output cavity. This serves to preserve the lens configuration of lens No. 4. The klystron will be tested in the beam analyzer with dc on the lenses and with the cathode pulsed. As it will be possible to apply rf input power to this tube, the beam characteristics will be tested with and without rf modulation. The pin hole target used to scan the beam is also mounted vertically. By means of electro-mechanical linkages, the target has freedom of movement vertically (z-axis) as well as horizontally (x-y axis). By means of an automatic scanning-recording system, it is possible to obtain a beam profile scan along any given transverse plane. In this manner, it will be possible to recognize beam instability and breakup as a function of rf drive.

The tube is being prepared for the beam analyzer at the time this report is being written.